EPJ Web of Conferences **130**, 01026 (2016) DOI: 10.1051/epjconf/201613001026
MESON 2016

Charmed meson production at LHCb

Dominik Müller[1,⋆]
for the LHCb Collaboration

[1] *School of Physics and Astronomy, The University of Manchester, Manchester, United Kingdom*

Abstract. Measurements of charm meson production are important tests for QCD predictions and LHCb is uniquely suited to perform these measurements in the forward region. This paper summarises recent charm meson production measurements performed by LHCb of J/ψ and open charm mesons and the associated production of Υ and open charm mesons. The J/ψ and open charm meson measurements are performed with data recorded in Run 2 of the Large Hadron Collider. With proton-proton collisions at $\sqrt{s} = 13\,\text{TeV}$, these open a new regime in which QCD predictions for charm meson production may be precisely tested. Furthermore, ratios of cross-sections at different centre-of-mass energies benefit of cancellation of both experimental and theoretical uncertainties, providing a new sensitive test of the QCD calculations. Measurements of Υ and open charm meson associated production are performed using $\sqrt{s} = 7\,\text{TeV}$ and $\sqrt{s} = 8\,\text{TeV}$ data and constitute the first observation of this production channel.

1 Introduction

Measurements of charm production cross-sections in proton-proton collisions are important tests of perturbative quantum chromodynamics [1–3], and LHCb can contribute unique measurements in the forward region. The LHCb detector is a single-arm forward spectrometer covering a pseudorapidity range of $2 < \eta < 5$ and is described in detail in Ref. [4, 5]. Recently, LHCb measured the production of J/ψ [6] and open charm mesons [7] at $\sqrt{s} = 13\,\text{TeV}$ and the associated production of Υ and open charm mesons at $\sqrt{s} = 7\,\text{TeV}$ and $\sqrt{s} = 8\,\text{TeV}$ [8]. This paper summarises these measurements.

Differential measurements of J/ψ and open charm meson production test the prediction of quantum chromodynamics to very high values of rapidity, y, and allow to probe a region where the momentum fraction, x, of the initial state partons can reach values below 10^{-4}. In this region the uncertainties on the gluon parton density functions are large, exceeding 30% [1, 9], and LHCb measurements can be used to constrain them. This is especially true for measurements of cross-section ratios between different center-of-mass energies which benefit from large cancellations in both theoretical and experimental uncertainties. Measurements of D^0, D^+, D_s^+, and $D^*(2010)^+$ (henceforth denoted as D^{*+}), generally referred to as D in the following, have previously been performed by the LHCb experiment at $\sqrt{s} = 7\,\text{TeV}$ [10] and of J/ψ at 2.76 TeV [11], 7 TeV [12] and 8 TeV [13].

Measurements of the associated production of two particles in the same pp interaction allow to study the contributions of different production mechanisms. Associated production can occur via

⋆e-mail: dominik.muller@cern.ch

single parton scattering (SPS) and double parton scattering (DPS). In the former, only one parton of each colliding proton interacts to produce both particles while in the latter, both particles are produced in independent parton interactions and the cross-section for the associated production approximately factorises. LHCb has previously measured the associated production of J/ψ and open charm mesons [14, 15] and the measured cross-sections significantly exceed the SPS expectations but agree with estimates for DPS.

2 Analysis strategy

The presented analyses reconstruct the final states $J/\psi \to \mu^-\mu^+$, $\Upsilon \to \mu^-\mu^+$, $D^0 \to K^-\pi^+$, $D^+ \to K^-\pi^+\pi^+$, $D_s^+ \to K^-K^+\pi^+$ and $D^{*+} \to D^0\pi^+$ with $D^0 \to K^-\pi^+$. A detailed description of the construction and selection of candidates as well the determination of the reconstruction and selection efficiencies is given in Refs [6–8]. In case of the associated production measurements, candidates for D and Υ mesons are treated separately with the exception that both must be consistent with originating from a common vertex. Differential cross-sections are then obtained from the relation

$$\frac{\mathrm{d}\sigma_i(M)}{\mathrm{d}a} = \frac{1}{\Delta a_i} \cdot \frac{N_i(M \to f + \text{c.c.})}{\varepsilon_{i,\text{tot}}(M \to f)\mathcal{B}(M \to f)\mathcal{L}_{\text{int}}}, \tag{1}$$

where M refers to any of the studied mesons or meson pairs, Δa_i are the widths of a bin i of the dependent variable a, $N_i(M \to f + \text{c.c.})$ is the measured signal yield for decays of M to the final state f in bin i plus the charge-conjugated decay, $\varepsilon_{i,\text{tot}}(M \to f)$ is the total efficiency for observing the signal decay in bin i, and $\mathcal{B}(M \to f)$ is the branching ratio of the decay to the specific final state, taken from Ref. [16]. The total integrated luminosity, $\mathcal{L}_{\text{int}}$, differs for the different sets of results presented here. The open charm meson measurement uses $5\,\text{pb}^{-1}$ and the J/ψ analysis $3\,\text{pb}^{-1}$ of 13 TeV data while the measurement of the associated production of D and Υ mesons uses $1\,\text{fb}^{-1}$ of 7 TeV and $2\,\text{fb}^{-1}$ of 8 TeV data.

3 Results for J/ψ production at 13 TeV

Results for J/ψ production in different J/ψ (p_T, y) bins are presented both for prompt production at the primary vertex (PV) of the pp collision as well as secondary J/ψ from the decay of heavier, long-lived particles (in the following referred to as from-b). The two contributions are separated from each other and from backgrounds in each (p_T, y) bin with a likelihood fit in the invariant dimuon mass $m(\mu^+\mu^-)$ and the measured decay time along the beam axis $t_z = (z_{J/\psi} - z_\text{PV})M_{J/\psi}/p_z$. As J/ψ decays instantaneously, the measured decay time for prompt J/ψ is compatible with 0 while the measured pseudo decay time for J/ψ from-b follows an exponential distribution consistent with the decay of long-lived b-hadrons.

The main measurements are the double differential cross-sections $\mathrm{d}^2\sigma/\mathrm{d}p_\text{T}\mathrm{d}y$ for prompt and from-b J/ψ which are given in Fig. 1. From these results, several additional results are derived, most notably single differential cross-sections integrated over y and their ratios between 13 TeV and 8 TeV [13]. Both of these are shown in Fig. 2 for prompt J/ψ and compared to theory predictions obtained from non-relativistic QCD calculations (NRQCD) [17]. Overall, the measured and predicted values are in agreement albeit the measured cross-sections are at the edge of the theory predictions, and the measured ratios are found to be consistently above the predictions. Furthermore, integrated cross-sections are computed for prompt and from-b J/ψ in the LHCb acceptance:

$$\begin{aligned} \sigma_\text{prompt} &= 15.30 \pm 0.03\,(\text{stat}) \pm 0.86\,(\text{sys})\ \mu\text{b and} \\ \sigma_\text{from-}b &= \ \ 2.34 \pm 0.01\,(\text{stat}) \pm 0.13\,(\text{sys})\ \mu\text{b}. \end{aligned} \tag{2}$$

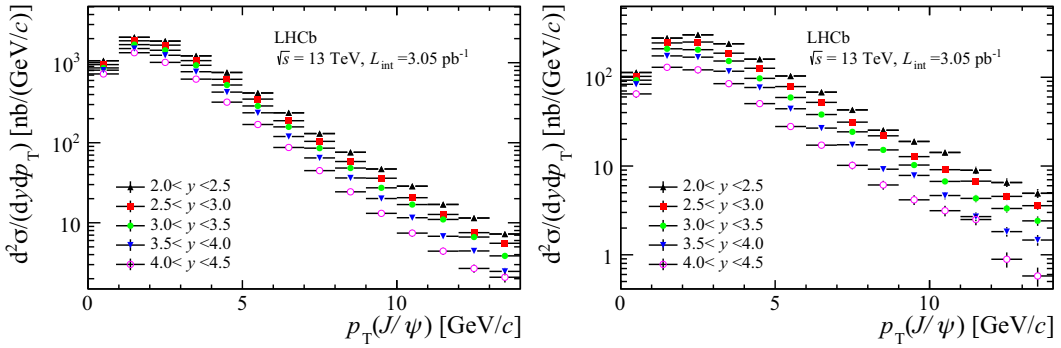

Figure 1: Measured double differential production cross-sections in p_T and y for prompt J/ψ (left) and J/ψ from-b (right).

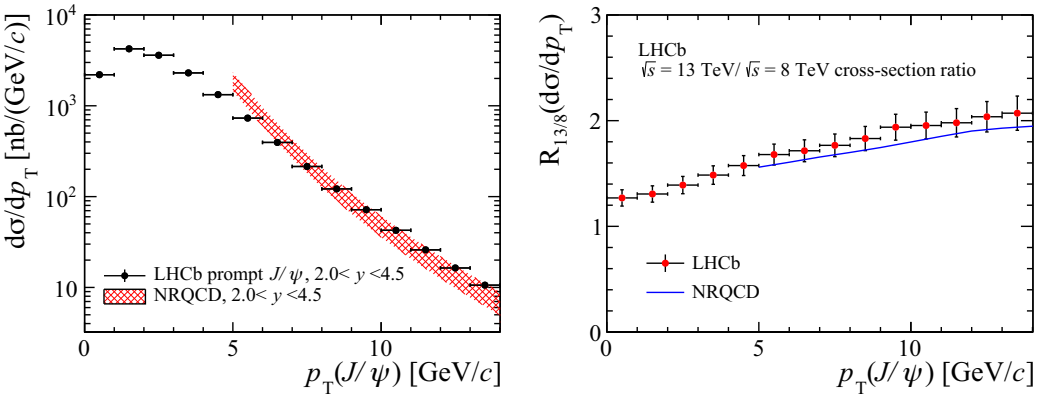

Figure 2: Production cross-sections in bins of p_T and integrated over $2 < y < 4.5$ for prompt J/ψ (left) and their ratios between 13 and 8 TeV (right). Also shown are NRQCD calculations [17].

4 Results for open charm production at 13 TeV

Results for open charm production at 13 TeV are obtained for charm mesons produced in the interaction vertex only. Secondary charm mesons are treated as background. To determine the number of promptly produced charm mesons, a two step fit is performed. The combinatorial background contamination is estimated and constrained from a fit to the invariant mass of the D candidate. Prompt and secondary contributions are then differentiated in a second fit to $\ln\chi^2_{\rm IP}$ where $\chi^2_{\rm IP}$ is defined as the difference in χ^2 of the reconstructed PV with and without the D candidate. As for J/ψ, the fit is performed in bins of (p_T, y) and the main results are again the differential cross-sections $d^2\sigma/dp_T dy$ measured in (p_T, y) bins. In the following, only results for $D^0 \to K^-\pi^+$ are shown and the full set of measurements are given in Ref. [7]. Fig. 3 shows the measured D^0 cross-section in (p_T, y) bins together with three sets of theory predictions [1–3]. Fig. 4 shows the cross-section ratios between 13 and 7 TeV for D^0 as well as the integrated cross-sections in the LHCb acceptance. Together, a similar pattern to the one seen in the J/ψ measurement emerges: the results are in agreement with the pre-

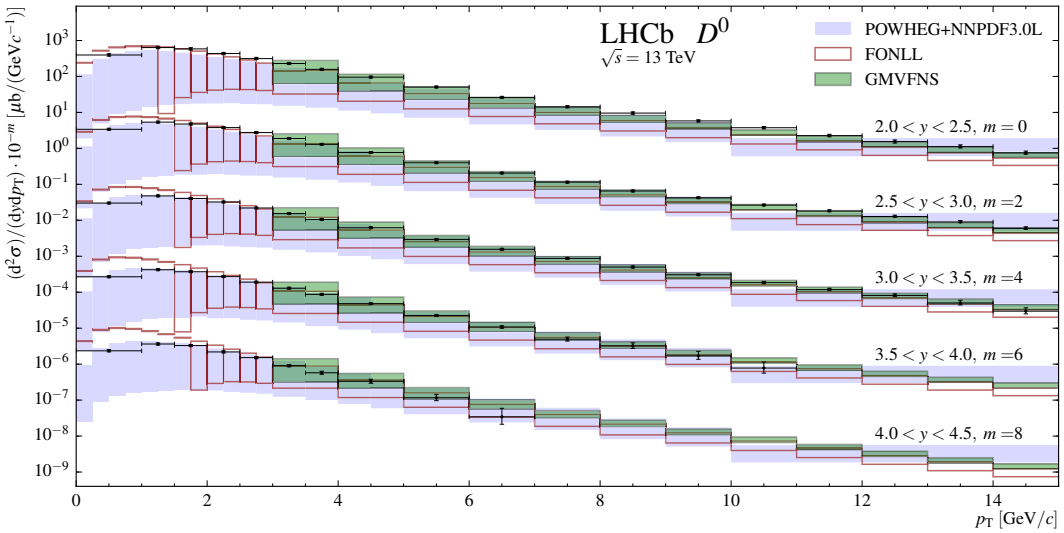

Figure 3: Differential D^0 cross-sections measured in (p_T, y) bins and compared with POWHEG+NNPDF3.0L [1], FONLL [2] and GMVFNS [3] predictions.

dictions though generally at the edge if the theoretical uncertainties. Using measured fragmentation fractions $f(c \to D)$ [18], estimates for the total $c\bar{c}$ cross-section are computed per meson species and averaged to obtain

$$\sigma(pp \to c\bar{c}X)_{p_T < 8\ \text{GeV/c},\, 2.0 < y < 4.5} = 2840 \pm 3\ (\text{stat}) \pm 170\ (\text{syst}) \pm 150\ (\text{frag})\ \mu\text{b}, \tag{3}$$

which is compared to theory predictions in Fig. 4.

5 Results for associated open charm and Υ production at 7 and 8 TeV

The total number of signal events is extracted from a two-dimensional likelihood fit to the invariant masses of the Υ and D candidates. The requirement that the Υ and D candidate must be consistent with originating from a common vertex significantly suppresses any contributions from secondary charm mesons and hence the yields obtained from the fit are assumed to be prompt. The results are limited by the sample size but constitute the first observation of $\Upsilon(1S)D^0$, $\Upsilon(2S)D^0$, $\Upsilon(1S)D^+$, $\Upsilon(2S)D^+$ and $\Upsilon(1S)D_s^+$ associated production with more than five standard deviations significance. For the $\Upsilon(1S)$ modes, the integrated production cross-sections are calculated:

$$\begin{aligned} \mathcal{B}(\Upsilon \to \mu^+\mu^-) \cdot \sigma_{7\,\text{TeV}}^{\Upsilon(1S)D^0} &= 155 \pm 21\ (\text{stat}) \pm\ \ 7\ (\text{sys})\ \text{pb and} \\ \mathcal{B}(\Upsilon \to \mu^+\mu^-) \cdot \sigma_{8\,\text{TeV}}^{\Upsilon(1S)D^0} &= 250 \pm 28\ (\text{stat}) \pm 11\ (\text{sys})\ \text{pb}. \end{aligned} \tag{4}$$

To estimate the relative contributions of SPS and DPS, the *${}_s\mathcal{P}lot$* technique is used to obtain background subtracted differential cross-section measurements. Fig. 5 shows the normalised cross-section as a function of $\Delta\phi$, the azimuthal angle between the D^0 and $\Upsilon(1S)$. The measured cross-section is in good agreement with the expected distribution for the DPS case, indicating that the SPS contribution,

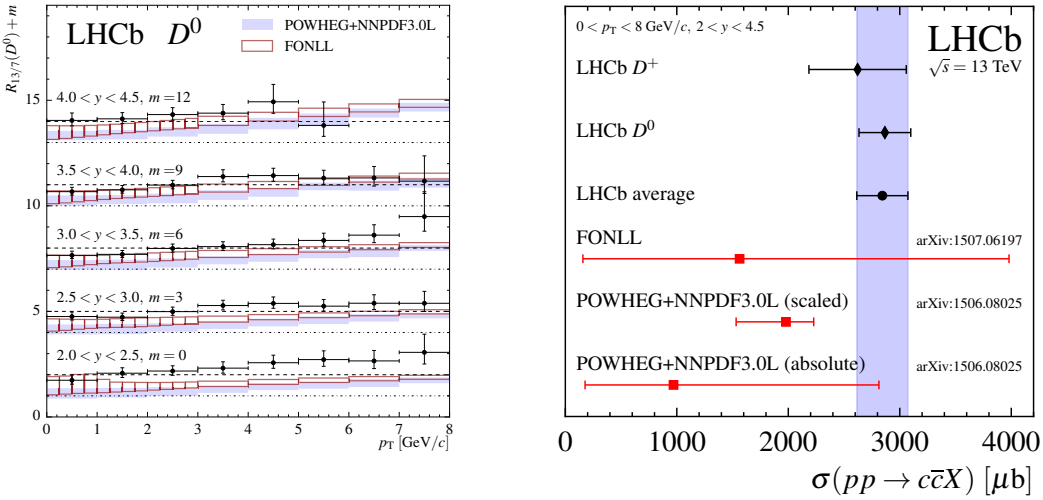

Figure 4: Ratio between D^0 cross-sections measurements at 13 and 7 TeV in (p_T, y) bins and integrated D^0 and D^+ cross-sections, both compared with POWHEG+NNPDF3.0L [1] and FONLL [2] predictions.

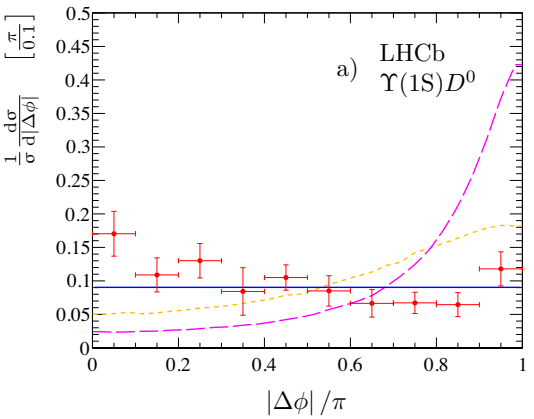

Figure 5: Normalised differential $\Upsilon(1S)D^0$ cross-section with respect to $\Delta\phi$, the difference in the azimuthal angles of $\Upsilon(1S)$ and D^0. The solid blue line shows a uniform distribution expected for uncorrelated production via DPS and the dashed magenta and orange lines show SPS calculations based on collinear approximation and k_T factorisation, respectively [8].

where an increase is expected for $\Delta\phi \approx \pi$, is small. In the DPS case, the cross-section factorises into the individual cross-sections:

$$\sigma(pp \to \Upsilon c\bar{c} + X) \approx \frac{\sigma(pp \to \Upsilon + X) \cdot \sigma(pp \to c\bar{c} + X)}{\sigma_{\text{eff}}}, \tag{5}$$

where σ_{eff} is an effective cross-section which provides the proper normalisation and is expected to be universal. To extract a value for σ_{eff}, the presented results for $\sigma(pp \to \Upsilon D + X)$ are divided by the fragmentation fractions to obtain $\sigma(pp \to \Upsilon c\bar{c} + X)$. Values for $\sigma(pp \to \Upsilon + X)$ and $\sigma(pp \to c\bar{c} + X)$ are taken from previous measurements [10, 19]. Averaging the individual results for ΥD^0 and ΥD^+ at both 7 and 8 TeV, the effective cross-section

$$\sigma_{\text{eff}} = 18.0 \pm 1.3\,(\text{stat}) \pm 1.2\,(\text{sys})\ \text{mb} \tag{6}$$

is computed and the result is in good agreement with previous measurements.

6 Summary

This paper summarises the recent production measurements of charm mesons at LHCb. Measured open charm and J/ψ production cross-sections at 13 TeV indicate an underestimation by the predictions for heavy-quark production, albeit the measurements are still within the theoretical uncertainties. The measurement of the associated production of open charm and Υ at 7 TeV and 8 TeV indicates that this process is dominated by the double parton scattering. Future measurements will benefit from the increased dataset available in Run 2 of the Large Hadron Collider and can potentially determine the fractions of SPS and DPS contributions.

References

[1] R. Gauld, J. Rojo, L. Rottoli, J. Talbert, JHEP **11**, 009 (2015)
[2] M. Cacciari, M.L. Mangano, P. Nason, Eur. Phys. J. **C75**, 610 (2015)
[3] B. Kniehl, G. Kramer, I. Schienbein, H. Spiesberger, Eur. Phys. J. **C72**, 2082 (2012)
[4] A.A. Alves Jr. et al. (LHCb collaboration), JINST **3**, S08005 (2008)
[5] R. Aaij et al. (LHCb collaboration), Int. J. Mod. Phys. **A30**, 1530022 (2015)
[6] R. Aaij et al. (LHCb collaboration), JHEP **10**, 172 (2015)
[7] R. Aaij et al. (LHCb collaboration), JHEP **03**, 159 (2016), Erratum-ibid **09**, 013 (2016)
[8] R. Aaij et al. (LHCb collaboration), JHEP **07**, 052 (2016)
[9] O. Zenaiev et al. (PROSA Collaboration), Eur. Phys. J. **C75**, 396 (2015)
[10] R. Aaij et al. (LHCb collaboration), Nucl. Phys. **B871**, 1 (2013)
[11] R. Aaij et al. (LHCb collaboration), JHEP **02**, 041 (2013)
[12] R. Aaij et al. (LHCb collaboration), Eur. Phys. J. **C71**, 1645 (2011)
[13] R. Aaij et al. (LHCb collaboration), JHEP **06**, 064 (2013)
[14] R. Aaij et al. (LHCb collaboration), Phys. Lett. **B707**, 52 (2012)
[15] R. Aaij et al. (LHCb collaboration), JHEP **06**, 141 (2012)
[16] K.A. Olive et al. (Particle Data Group), Chin. Phys. **C38**, 090001 (2014), and 2015 update
[17] H.S. Shao, H. Han, Y.Q. Ma, C. Meng, Y.J. Zhang, K.T. Chao, JHEP **2015**, 1 (2015)
[18] C. Amsler et al. (Particle Data Group), Phys. Lett. **B667**, 1 (2008)
[19] R. Aaij et al. (LHCb collaboration), JHEP **11**, 103 (2015)